RESEARCH ARTICLE

DFT Studies on the Sulfamethoxazole Interactions with C_8B_6N6 Nanocluster

Pedram Niknam Rad[1], Mahnaz Qomi[2,3], Mohammad Reza Jalali Sarvestani[4,*]

[1] Department of Chemistry, Faculty of Science Hamedan Branch, Islamic Azad University, Hamedan, Iran

[2] Active Pharmaceutical Ingredients Research Center (APIRC), Tehran Medical Sciences, Islamic Azad University, Tehran, Iran

[3] Department of Medicinal Chemistry, Faculty of Pharmacy, Tehran Medical Sciences, Islamic Azad University, Tehran, Iran

[4] Young Researchers and Elite Club, Yadegar-e-Imam Khomeini (RAH) Shahr-e-Rey Branch, Islamic Azad University, Tehran, Iran

ARTICLE INFO

Article History:
Received 27 Mar 2024
Accepted 19 May 2024
Published 01 Jul 2024

Keywords:
Sulfamethoxazole
Adsorption
Nanocluster
Antibiotic resistance
DFT simulations

ABSTRACT

The research carried out an inquiry into the efficiency of $C_8B_6N_6$ nanoclusters as both an adsorbent and a sensor for the elimination and identification of sulfamethoxazole (SMZ) using density functional theory computations. The results of the study showed that the interaction between SMZ and $C_8B_6N_6$ is not only possible but also releases heat and occurs naturally, indicating the potential of $C_8B_6N_6$ as a very effective adsorbent for eliminating SMZ. Additionally, the study explored the impact of water as the solvent and different temperatures on the thermodynamic parameters, ultimately revealing that these factors did not have a significant effect on the connections. Moreover, the analysis of Frontier Molecular Orbital (FMO) uncovered significant alterations in the bandgap of $C_8B_6N_6$, from 8.101 (eV) to 4.875 (eV) (-40.933%) during the adsorption process, hinting at its likelihood to be a helpful electrocatalytic modifier for the electrochemical detection of SMZ. The study also thoroughly examined several other FMO parameters. In conclusion, this investigation offers valuable insights into the promising capabilities of $C_8B_6N_6$ as a highly effective adsorbent and sensor for the elimination and detection of SMZ.

How to cite this article
Niknam Rad P., Qomi M., Jalali Sarvestani M.R. DFT Studies on the Sulfamethoxazole Interactions with $C_8B_6N_6$ Nanocluster. Nanomed Res J, 2024; 9(2): 206-212. DOI: 10.22034/nmrj.2024.02.009

INTRODUCTION

Sulfamethoxazole (SMZ, Fig.1) is a widely used antibiotic that belongs to the class of sulfonamides [1]. It is commonly used to treat various bacterial infections such as urinary tract infections, bronchitis, and ear infections. However, over the years, there has been a growing concern about the increasing resistance to SMZ among bacteria [2]. Resistance to SMZ occurs when bacteria develop mechanisms to evade the effects of the antibiotic [3]. This can happen through various ways, such as the production of enzymes that inactivate the drug, mutations in the bacterial target site that reduces the binding affinity of the antibiotic, or the acquisition of genes that confer resistance [4]. The misuse and overuse of SMZ in both human and veterinary medicine have contributed to the emergence of resistant bacterial strains [5]. The importance of addressing resistance to SMZ cannot be overstated. Antibiotic resistance poses a significant threat to public health, as it limits the effectiveness of treatment options and can lead to prolonged illness, increased healthcare costs, and higher mortality rates [6]. In the case of SMZ, its resistance can compromise the ability to effectively manage common bacterial infections, leading to treatment failures and the need for alternative, often more expensive and less accessible antibiotics [7]. Efforts to mitigate resistance to SMZ involve a multifaceted approach. This includes promoting responsible use of the antibiotic in both clinical

* Corresponding Author Email: rezajalali93@yahoo.com

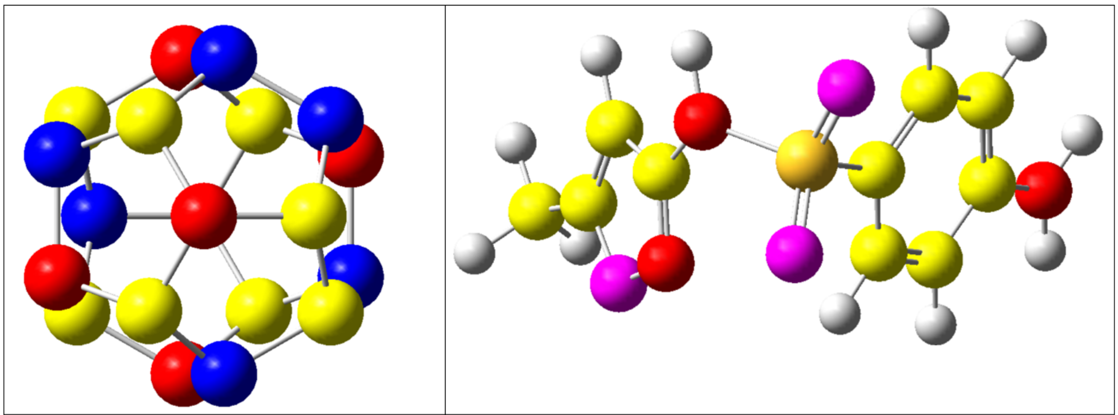

$C_8B_6N_6$	SMZ

Fig. 1. The structures of nanocluster ($C_8B_6N_6$) and SMZ (blue: boron, greenish yellow: sulphur, yellow: carbon, white: hydrogen, purple: oxygen red: nitrogen,)

and agricultural settings, as well as improving surveillance and monitoring of resistance patterns [8]. Additionally, research into the development of new antibiotics and alternative treatment strategies is crucial to address the growing threat of resistance [9]. Furthermore, the removal of SMZ from the environment is also of paramount importance [10]. The presence of SMZ in wastewater and surface water can contribute to the selection and spread of resistant bacteria [10]. This is due to the fact that sub-lethal concentrations of antibiotics in the environment can exert selective pressure on bacteria, favoring the survival and proliferation of resistant strains [11]. Therefore, proper wastewater treatment and the implementation of advanced technologies for the removal of SMZ from water sources are essential to minimize the impact of antibiotic resistance [12]. Adsorptive removal presents multiple advantages over alternative contaminant removal methods [13]. It is highly effective in removing a wide range of pollutants from water and air, including organic and inorganic compounds, heavy metals, and pathogens [14]. This approach is cost-effective, sustainable, and easily adaptable for various application scales [15]. Overall, adsorptive removal is a valuable solution for addressing pollution challenges in water and air treatment, and it is likely to become increasingly important in environmental remediation efforts as technology advances [16]. The $C_8B_6N_6$ (Fig. 1) nanocluster is a unique and promising material that has garnered significant attention in the field of nanotechnology [17]. Comprised of carbon, boron, and nitrogen atoms, this nanocluster exhibits exceptional properties that make it a potential candidate for various applications [18-20]. One of the most intriguing aspects of the $C_8B_6N_6$ nanocluster is its structural stability and electronic properties [21-24]. The arrangement of carbon, boron, and nitrogen atoms within the nanocluster results in a highly stable configuration, allowing it to withstand harsh environmental conditions and maintain its structural integrity [25-27]. Additionally, the electronic structure of the $C_8B_6N_6$ nanocluster gives rise to desirable properties such as high conductivity and unique optical characteristics, making it an attractive material for use in electronic and photonic devices [28, 29]. Furthermore, the $C_8B_6N_6$ nanocluster has shown promise in catalytic applications. Its unique surface properties and reactivity make it a potential candidate for catalyzing various chemical reactions, offering opportunities for efficient and sustainable processes in areas such as energy production and environmental remediation [30]. In addition to its structural and electronic properties, the $C_8B_6N_6$ nanocluster also exhibits potential in biomedical applications. Its biocompatibility and ability to interact with biological systems make it a promising candidate for drug delivery and imaging applications, offering new possibilities for targeted therapies and diagnostic techniques. In this respect, the applicability of $C_8B_6N_6$ nanocluster as an adsorbent and sensor for the removal and detect of SMZ was scrutinized in this research, for the first time.

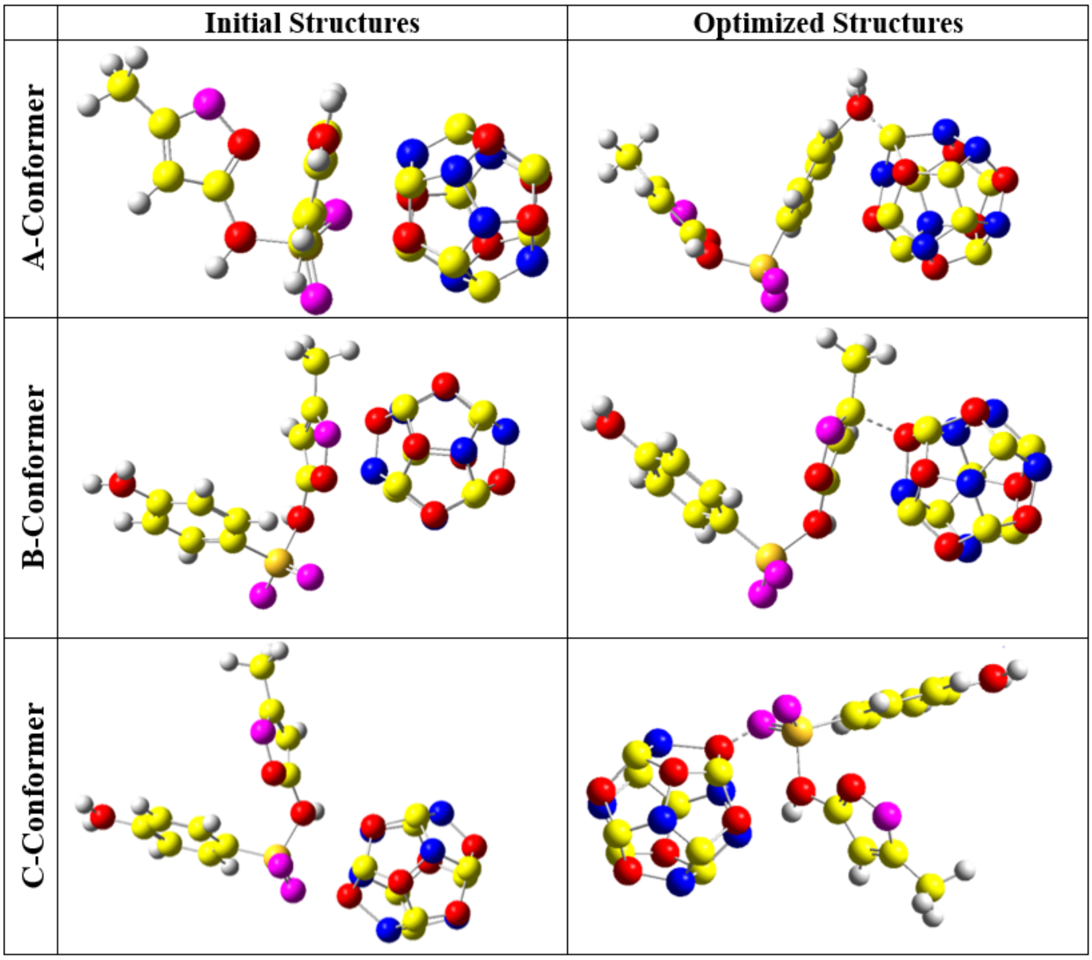

Fig. 2. The initial and optimized structures of nanocluster ($C_8B_6N_6$) and SMZ complexes (blue: boron, greenish yellow: sulphur, yellow: carbon, white: hydrogen, purple: oxygen, red: nitrogen)

COMPUTATIONAL DETAILS

The specific process scrutinized was the interaction between SMZ and the adsorbent, leading to the formation of SMZ-Adsorbent complex as represented by the equation:

SMZ + Adsorbent → SMZ-Adsorbent (1)

The calculated factors were computed by the procedures outlined in [30-40].

RESULTS AND DISCUSSION

This study focused on investigating the structures and interaction of the SMZ-C8B6N6 complexes. Figure 2 displays the initial and optimized configurations of these complexes. The main objective of the research was to identify the most stable arrangement among three distinct configurations: A-Conformer, B-Conformer, and C-Conformer. In the A-Conformer, the nanostructure is positioned near the benzene ring of SMZ, with a parallel orientation. Likewise, the B-Conformer situates the adsorbent in close proximity to the methyl isoxazole ring of SMZ, also in a parallel orientation. In contrast, the C-Conformer situates the adsorbent near the aliphatic chain of SMZ. After geometrical optimization, it was observed that the adsorbate shifted noticeably towards the adsorbent in all configurations, indicating a significant level of interaction between the two [33]. This analysis offers valuable insights into the interaction between SMZ and C8B6N6, providing understanding of the preferred configurations and the nature of their bonding. These findings enhance knowledge of molecular interactions at the nanoscale, with

Table 1. Structural properties of SMZ, $C_8B_6N_6$ and their complexes

NO	Adsorption energy (kJ/mol)	Zero-point energy (kJ/mol)	ν_{min} (cm^{-1})	ν_{max} (cm^{-1})	Dipole moment (Deby)
SMZ (Vacuum)	---	702.027	44.125	4221.450	1.890
SMZ (Water)	---	704.322	44.366	4319.635	2.120
$C_8B_6N_6$ (Vacuum)	---	285.853	374.992	1643.391	0.000
$C_8B_6N_6$ (Water)	---	295.319	376.376	1639.742	0.020
A-Conformer (Vacuum)	-78.790	1098.466	20.331	3770.363	5.480
A-Conformer (Water)	-64.535	1103.166	22.050	3771.003	6.110
B-Conformer (Vacuum)	-43.029	1115.133	13.469	4224.244	7.120
B-Conformer (Water)	-31.527	1099.820	14.308	4226.491	8.090
C-Conformer (Vacuum)	-105.194	1104.320	13.692	4309.409	9.010
C-Conformer (Water)	-86.302	1108.622	16.161	4311.479	9.980

potential implications for various applications in materials science and nanotechnology. The findings in Table 1 consistently show that the adsorption energies are negative, indicating that the adsorption process is feasible under experimental conditions [34]. Additionally, a thorough analysis of the impact of water as a solvent on the adsorption energies has revealed that it does not significantly affect the underlying interactions [35]. This discovery highlights the resilience of the adsorption process, regardless of the presence of water as a solvent. Upon closer examination, it is clear that the presence of water has minimal impact on the modification of adsorption energies. These results contribute to our understanding of the adsorption process and its ability to withstand various solvent environments. After undergoing geometric optimizations, the structure underwent IR computations, leading to the identification of both minimum and maximum frequencies as outlined in Table 1. All calculated frequencies showed positive values, indicating that the structures scrutinized represent verified local minima. This result confirms the stability of the analyzed structures [36]. Moreover, Table 1 presents dipole moment values, unveiling noteworthy fluctuations in the dipole moment subsequent to the adsorption of SMZ onto the $C_8B_6N_6$ surface. This finding implies a substantial improvement in the solubility and chemical reactivity of SMZ when it is adsorbed on the nanocluster [37]. Within the various configurations examined, the C-Conformer demonstrated the most negative adsorption energy value, indicating that the formation of this arrangement is more preferable than others.

The thermodynamic parameters presented in Table 2 reveal a notable exothermic and spontaneous interaction between SMZ and $C_8B_6N_6$, as indicated by the negative values of ΔH_{ad} and ΔG_{ad} [40]. This suggests that the interaction between the two compounds releases heat and occurs without external influence. Additionally, the study delved into the effects of temperature and solvent on these interactions and determined that neither factor had a significant impact on the thermodynamic parameters [39]. This implies that the nature of the interaction remains consistent across a range of temperatures and in various solvents. Of particular interest are the negative values of ΔSad, indicating that the adsorption process is unfavorable in terms of entropy [38]. This suggests that there is a decrease in disorder or randomness during the adsorption process, potentially leading to the aggregation of nanostructures after the drug adsorption. This insight into the thermodynamic parameters provides valuable information regarding the nature of the interaction between SMZ and $C_8B_6N_6$, shedding light on the underlying processes at play. In conclusion, the thermodynamic analysis reveals important characteristics of the interaction between SMZ and C8B6N6, highlighting its exothermic and spontaneous nature, as well as the impact of temperature and solvent. The unfavorable entropy change observed during the adsorption process offers intriguing implications for the aggregation of nanostructures. This comprehensive understanding of the thermodynamic parameters enriches our knowledge of these interactions and paves the way for further exploration in this field.

Table 2. The calculated Thermodynamic parameters

NO	ΔH_{ad} (kJ/mol)	ΔG_{ad} (kJ/mol)	ΔS_{ad} (J/mol)
A-Conformer-Vacuum-298	-99.501	-43.380	-182.132
A-Conformer-Vacuum-308	-97.702	-37.511	-184.691
A-Conformer-Vacuum-318	-95.909	-31.642	-187.253
A-Conformer-Water-298	-6.524	-43.386	-176.344
A-Conformer-Water-308	-4.720	-36.265	-178.906
A-Conformer-Water-318	-2.921	-29.147	-182.462
B-Conformer-Vacuum-298	-67.306	-16.594	-163.940
B-Conformer-Vacuum-308	-65.500	-12.607	-166.501
B-Conformer-Vacuum-318	-63.702	-8.620	-169.069
B-Conformer-Water-298	-55.804	-5.092	-174.453
B-Conformer-Water-308	-54.009	-3.184	-172.310
B-Conformer-Water-318	-52.203	-1.276	-174.879
C-Conformer-Vacuum-298	-124.900	-68.790	-176.984
C-Conformer-Vacuum-308	-123.105	-65.579	-179.543
C-Conformer-Vacuum-318	-121.301	-62.368	-182.109
C-Conformer-Water-298	-115.011	-68.790	-170.130
C-Conformer-Water-308	-113.218	-63.378	-172.697
C-Conformer-Water-318	-111.413	-57.966	-175.256

Table 3. The calculated FMO parameters

NO	E_{HOMO} (eV)	E_{LUMO} (eV)	Eg (eV)	%ΔEg	η (eV)	μ (eV)	ω (eV)	ΔNmax (eV)
SMZ	-7.731	4.376	12.107	---	6.054	-0.678	0.038	0.112
$C_8B_6N_6$	-5.629	2.472	8.101	---	4.051	-1.579	0.308	0.390
A-Conformer	-3.456	1.329	4.785	-40.933	2.393	-1.064	0.236	0.445
B-Conformer	-4.987	2.190	7.177	-11.406	3.589	-1.399	0.273	0.390
C-Conformer	-4.567	1.876	6.443	-20.467	3.222	-1.346	0.281	0.418

The results displayed in Table 3 offer compelling evidence of the significant impact of SMZ adsorption on the properties of $C_8B_6N_6$. It is apparent that the bandgap of $C_8B_6N_6$ undergoes a marked shift from 8.101 eV to 7.177, 6.443, and 6.433 eV for A, B, and C conformers, respectively, indicating a substantial change in bandgap during the adsorption process. This finding strongly suggests that the assessed nanocluster has the potential to effectively alter the electrocatalytic detection of SMZ. Additionally, it is important to note that the chemical hardness of SMZ notably decreases upon interaction with $C_8B_6N_6$, indicating enhanced chemical reactivity. The identification of negative values for the chemical potential further supports the thermodynamic stability of the structures being studied. Moreover, upon interaction with the $C_8B_6N_6$ surface, SMZ displays a marked increase in both electrophilicity and maximum transferred charge capacity, indicating a heightened tendency for electron absorption. In essence, these results suggest that SMZ-$C_8B_6N_6$ complexes exhibit greater chemical reactivity compared to pure SMZ in the absence of a nanostructure.

CONCLUSION

The study conducted an in-depth analysis of the efficacy of $C_8B_6N_6$ nanocluster as both an adsorbent and sensor for the purpose of removing and detecting sulfamethoxazole (SMZ) using density functional theory computations. The findings of the research revealed a viable, exothermic, and spontaneous interaction between SMZ and $C_8B_6N_6$, indicating the potential of $C_8B_6N_6$ as an efficient adsorbent for the removal of SMZ. Moreover, the investigation into the influence of water as the solvent and varying temperature on the thermodynamic parameters demonstrated that these factors did not have a significant impact on the interactions. Additionally, the Frontier Molecular Orbital (FMO) analysis uncovered notable changes in the bandgap of $C_8B_6N_6$ during the adsorption process, suggesting its potential utility as an effective electrocatalytic modifier for the electrochemical detection of SMZ. The study also delved into a detailed discussion of other FMO parameters. In conclusion, this study offers valuable insights into the potential use of $C_8B_6N_6$ as an efficient adsorbent and sensor for the removal and detection of SMZ.

CONFLICT OF INTEREST

The authors declare no conflict of interest.

REFERENCES

1. Dutta J, Mala AA. Removal of antibiotic from the water environment by the adsorption technologies: a review. Water. Sci. Technol., 2020;82(3):401-26. https://doi.org/10.2166/wst.2020.335
2. Du C, Zhang Z, Yu G, Wu H, Chen H, Zhou L, Wang S. A review of metal organic framework (MOFs)-based materials for antibiotics removal via adsorption and photocatalysis. Chemosphere, 2021;272(12):129501. https://doi.org/10.1016/j.chemosphere.2020.129501
3. Mangla D, Sharma A, Ikram S. Critical review on adsorptive removal of antibiotics: Present situation, challenges and future perspective. J. Hazard. Mater., 2022;425:127946. https://doi.org/10.1016/j.jhazmat.2021.127946
4. Ahmed MB, Zhou JL, Ngo HH, Guo W. Adsorptive removal of antibiotics from water and wastewater: Progress and challenges. Sci. Total. Environ., 2015;532:112-26. https://doi.org/10.1016/j.scitotenv.2015.05.130
5. Yu F, Li Y, Han S, Ma J. Adsorptive removal of antibiotics from aqueous solution using carbon materials. Chemosphere, 2016;153:365-85. https://doi.org/10.1016/j.chemosphere.2016.03.083
6. Juela DM. Promising adsorptive materials derived from agricultural and industrial wastes for antibiotic removal: a comprehensive review. Sep. Purif. Technol., 2022;284:120286. https://doi.org/10.1016/j.seppur.2021.120286
7. Nguyen LM, Nguyen NTT, Nguyen DTC, Tran TV. Occurrence, toxicity and adsorptive removal of the chloramphenicol antibiotic in water: a review. Environ. Chem. Lett., 2022; 20(3):1929-63. https://doi.org/10.1007/s10311-022-01416-x
8. Li MF, Liu YG, Zeng GM, Liu N, Liu SB. Removal of tetracycline and oxytetracycline from water by magnetic Fe3O4@graphene. Chemosphere, 2019;226:360-80. https://doi.org/10.1016/j.chemosphere.2019.03.117
9. Eniola JO, Kumar R, Barakat MA. Adsorptive removal of antibiotics from water over natural and modified adsorbents. Environ. Sci. Pollut. Res., 2019;26:34775-88. https://doi.org/10.1007/s11356-019-06641-6
10. Zhou L, Li N, Owens G, Chen Z. Simultaneous removal of mixed contaminants, copper and norfloxacin, from aqueous solution by ZIF-8. Chem.Eng. J., 2019;362:628-37. https://doi.org/10.1016/j.cej.2019.01.068
11. Chierentin L, Salgado HRN. Review of Properties and Analytical Methods for the Determination of Norfloxacin Crit. Rev. Anal. Chem., 2016;46(1):22-39.Safari GH, Nasseri S, Mahvi AH, Yaghmaeian K, Nabizadeh R, Alimohammadi M. Optimization of sonochemical degradation of tetracycline in aqueous solution using sono-activated persulfate process. J. Environ. Health Sci. Eng., 2015;13:76. https://doi.org/10.1186/s40201-015-0234-7
12. Foureaux AFS, Reis EO, Lebron Y, Moreira V, Santos LV, Amaral MS, Lange LC. Rejection of pharmaceutical compounds from surface water by nanofiltration and reverse osmosis. Sep. Purif. Technol.,2019;212:171-179. https://doi.org/10.1016/j.seppur.2018.11.018
13. Zhu J, Lu Z, Jing X, Wang X, Liu Q, Wu L. Adsorption of temozolomide chemotherapy drug on the pristine BC3NT: quantum chemical study. Chem Pap, 2020;74:4525-4531. https://doi.org/10.1007/s11696-020-01232-z
14. Zhao H, Hou S, Zhao X, Liu D. Adsorption and pH-responsive release of tinidazole on metal-organic framework CAU-1. J Chem Eng Data, 2019;64:1851-1858. https://doi.org/10.1021/acs.jced.9b00106
15. Miller TW, Siringan FP, Tanabe S. Determination of preservative and antimicrobial compounds in fish from Manila Bay, Philippines using ultra high performance liquid chromatography tandem mass spectrometry, and assessment of human dietary exposure. J. Hazard. Mater., 2011;192 (3):1739-1745. https://doi.org/10.1016/j.jhazmat.2011.07.006
16. Alnajjar A, AbuSeada HH, Idris AM. Capillary electrophoresis for the determination of norfloxacin and tinidazole in pharmaceuticals with multi-response optimization. Talanta, 2007;72(2):842-6. https://doi.org/10.1016/j.talanta.2006.11.025
17. Lopez-Darias J, Pino V, Meng Y, Anderson JL, Afonso AM. Utilization of a benzyl functionalized polymeric ionic liquid for the sensitive determination of polycyclic aromatic hydrocarbons; parabens and alkylphenols in waters using solid phase microextraction coupled to gas chromatography-flame ionization detection. J. Chromatogr. A., 2010;1217(46):7189-7197. https://doi.org/10.1016/j.chroma.2010.09.016
18. Ioannidi A, Frontistis Z, Mantzavinos D. Destruction of propyl paraben by persulfate activated with UV-A light emitting diodes. J. Environ. Chem. Eng., 2018;6:2992-2997. https://doi.org/10.1016/j.jece.2018.04.049
19. Goyal RN, Rana ARS, Chasta H. Electrochemical sensor for the sensitive determination of norfloxacin in human urine and pharmaceuticals. Bioelectrochemistry, 2012;83:46-51. https://doi.org/10.1016/j.bioelechem.2011.08.006
20. Privett BJ, Shin JH, Schoenfisch MH. Electrochemical Sensors. Anal. Chem., 2010;82(12):4723-41. https://doi.org/10.1021/ac101075n
21. Radovan C, Cinghită D, Manea F, Mincea M, Cofan C, Ostafe V. Electrochemical sensing and assessment of parabens in hydro-alcoholic solutions and water using a boron-doped diamond electrode. Sensors, 2008;8(7):4330-4349. https://doi.org/10.3390/s8074330
22. Hamnca S, Phelane L, Iwuoha E, Baker P. Electrochemical Determination of Neomycin and Norfloxacin at a Novel Polymer Nanocomposite Electrode in Aqueous Solution. Anal. Lett., 2017;50(12):1887-96. https://doi.org/10.1080/00032719.2016.1261876
23. Jalali Sarvestani MR, Majedi S. A DFT study on the interaction of alprazolam with fullerene (C20). Chem Lett.,2020;1:32-38.
24. Doroudi Z, Jalali Sarvestani MR. Boron nitride nanocone as an adsorbent and senor for Ampicillin: a computational study. Chem Rev Lett., 2020;3:110-116.
25. Ahmadi R, Jalali Sarvestani MR. Adsorption of Tetranitrocarbazole on the Surface of Six Carbon-Based Nanostructures: A Density Functional Theory Investigation.

Russ. J. Phys. Chem. B., 2020;14(1):198-208. https://doi.org/10.1134/S1990793120010194
26. Shahzad H, Ahmadi R, Adhami F, Najafpour J. Adsorption of Cytarabine on the Surface of Fullerene C20: A Comprehensive DFT Study. Eurasian Chem Commun, 2020;2:162-169. https://doi.org/10.33945/SAMI/ECC.2020.2.1
27. Tang C, Zhu W, Zou H, Zhang A, Gong J, Tao C (2012) Density functional study on the electronic properties, polarizabilities, NICS values, and absorption spectra of fluorinated fullerene derivative C60F17CF3. Comput Theor Chem., 2012;991:154-160. https://doi.org/10.1016/j.comptc.2012.04.015
28. Elhaes H, Ibrahim M. Fullerene as sensor for halides: modeling approach. J Comput Theor Nanosci., 2013;10:2026-2028. https://doi.org/10.1166/jctn.2013.3164
29. GaussView, Version 6.1, Dennington R, Todd K, and John M. Semichem Inc., Shawnee Mission, KS, 2016.
30. Melchor S, Dobado JA. CoNTube: An Algorithm for Connecting Two Arbitrary Carbon Nanotubes. Journal of Chemical Information and Computing Science, 2004;44(5):1639-1646. https://doi.org/10.1021/ci049857w
31. Gaussian 16, Revision B.01, Frisch MJ, Trucks GW, Schlegel HB, Scuseria GE, Robb MA, Cheeseman JR, Scalmani G, Barone V, Petersson GA, Nakatsuji H, Li X, Caricato M, Marenich AV, Bloino J, Janesko BG, Gomperts R, Mennucci B, Hratchian HP, Ortiz JV, Izmaylov AF, Sonnenberg JL, Williams-Young D, Ding F, Lipparini F, Egidi F, Goings J, Peng B, Petrone A, Henderson T, Ranasinghe D, Zakrzewski VG, Gao J, Rega N, Zheng G, Liang W, Hada M, Ehara M, Toyota K, Fukuda R, Hasegawa J, Ishida M, Nakajima T, Honda Y, Kitao O, Nakai H, Vreven T, Throssell K, Montgomery Jr, Peralta JA, Ogliaro JE, Bearpark F, Heyd MJ, Brothers JJ, Kudin EN, Staroverov KN, Keith VN, Kobayashi TA, Normand R, Raghavachari J, Rendell K, Burant AP, Iyengar JC, Tomasi SS, Cossi J, Millam M, Klene JM, Adamo M, Cammi C, Ochterski R, Martin JW, Morokuma RL, Farkas K, Foresman O, Fox JB, Gaussian, DJ. Inc., Wallingford CT, 2016; GaussView 5.0. Wallingford, E.U.A.
32. Hassani, B., Karimian, M., Ghoreishi Amin, N. DFT Studies on 10 Chromenes Derivatives Performance as Sensing Materials for Electrochemical Detection of Lithium (I). Int. J. New. Chem., 2024; 11(3): 204-215.
33. Tayebi-Moghaddam S, Aliakbari M, Tayeboun K. Fullerene (C24) as a Potential Sensor for the Detection of Acrylamide: A DFT study. Int. J. New. Chem.,2023;11(2):82-89.
34. Rezaei Sameti M, Barandisheh Naghibi M. A quantum assessment of the interaction between Si12C12, BSi11C12, BSi12C11, NSi11C12 and NSi12C11 nanocages with Glycine amino acid: A DFT, TD-DFT and AIM study. Int. J. New. Chem., 2024;11(1):15-33.
35. Abrahi Vahed S, Hemmati Tirabadi F.Carbon Nanocone as a Potential Adsorbent and Sensor for the Removal and Detection of Ciprofloxacin: DFT Studies. Int. J. New. Chem., 2023;10(4):288-298.
36. Mohammad Alipour F, Babazadeh M, Vessally E, Hosseinian A, Delir Kheirollahi Nezhad P. Theoretical study of some graphene-Like nanoparticles as the anodes in K–ion Batteries. Int. J. New. Chem., 2023;10(3):197-212.
37. Farahani R, Madrakian T, Afkhami A. Investigating the performance of a recently synthesized covalent organic framework as an adsorbent for methylene blue: A DFT Study. Int. J. New. Chem., 2023;9(4):383-392.
38. Takano Y, Houk KN. Benchmarking the conductor-like polarizable continuum model (CPCM) for aqueous solvation free energies of neutral and ionic organic molecules. Journal of Chemical Theory and Computation, 2005;1(1):70-77. https://doi.org/10.1021/ct049977a
39. Jalali Sarvestani MR, Abrahi Vahed S, Ahmadi R. Cefalexin adsorption on the surface of pristine and Al-doped boron nitride nanocages (B12N12 and AlB11N12): A theoretical study. S. Afr. J. Chem. Eng., 2024; 47:60-66. https://doi.org/10.1016/j.sajce.2023.10.008
40. Jalali Sarvestani MR, Qomi M, Arabi S. Norfloxacin Adsorption on the Surface of B12N12 and Al12N12 Nanoclusters: A Comparative DFT Study Nanomed. Res. J., 2023; 8(4), 393-400.